The Journal of Physical Chemistry Letters

Physical Insights into Light Interacting with Matter

On the Origin of the Photostability of DNA and RNA Monomers: Excited State Relaxation Mechanism of the Pyrimidine Chromophore

Enrique Manuel Arpa, Matthew M Brister, Sean J. Hoehn, Carlos E. Crespo-Hernández, and Ines Corral

J. Phys. Chem. Lett., **Just Accepted Manuscript** • DOI: 10.1021/acs.jpclett.0c00935 • Publication Date (Web): 05 Jun 2020

On the Origin of the Photostability of DNA and RNA Monomers: Excited State Relaxation Mechanism of the Pyrimidine Chromophore

Enrique M. Arpa[1,¶] , Matthew M. Brister[2,3¶], Sean J. Hoehn[2], Carlos E. Crespo-Hernández[2,*], Inés Corral[1,4,*]

[1]Departamento de Química. Facultad de Ciencias. Universidad Autónoma de Madrid. C/ Francisco Tomás y Valiente 7, 28049 Madrid, España.
[2]Department of Chemistry, Case Western Reserve University, 10900 Euclid Ave., Cleveland, Ohio 44106, United States.
[3]Current Address: Lawrence Berkeley National Laboratory, Atomic Molecular and Optical Sciences, Chemical Science Division, Berkeley, CA 94720, United States.
[4]Institute of Advanced Research in Chemical Sciences (IAdChem). Universidad Autónoma de Madrid. C/ Francisco Tomás y Valiente 7, 28049 Madrid, España.

¶ these authors contributed equally to this work; * corresponding authors: carlos.crespo@case.edu; ines.corral@uam.es.

ABSTRACT

Today's genetic composition is the result of continual refinement processes on primordial heterocycles present in prebiotic Earth and at least partially regulated by ultraviolet radiation. Femtosecond transient absorption spectroscopy and state-of-the-art ab initio calculations are combined to unravel the electronic relaxation mechanism of pyrimidine—the common chromophore of the nucleobases. Excitation of pyrimidine at 268 nm populates the $S_1(n\pi^*)$ state directly. A fraction of the population intersystem crosses to the triplet manifold within 7.8 ps, partially decaying within 1.5 ns, while another fraction recovers the ground state in >3 ns. The pyrimidine chromophore is not responsible for the photostability of the nucleobases. Instead, C2 and C4 amino and/or carbonyl functionalization is essential for shaping the topography of pyrimidine's potential energy surfaces, which present accessible conical intersections between the initially populated electronic excited state and the ground state.

TOC

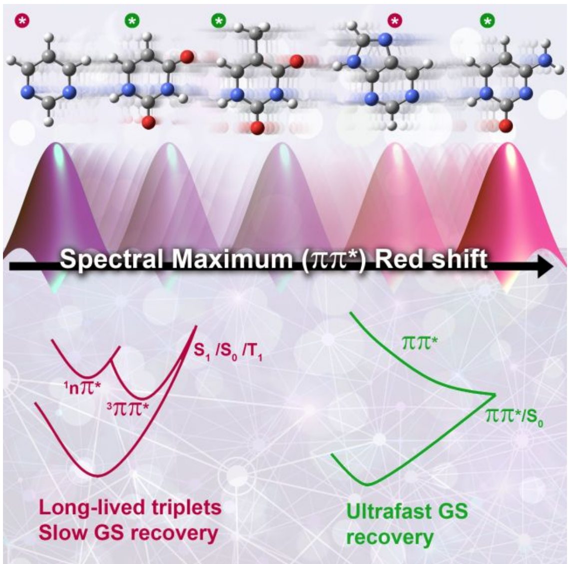

Keywords: chemical origin of life, DNA/RNA nucleobases, photostability, intersystem crossing, ab initio calculations, transient absorption spectroscopy.

Investigating the origin of the photostability of the DNA and RNA nucleobases is a paramount step toward understanding the molecular origin of life on Earth. For decades, an extraordinary amount of effort has been dedicated to investigate and understand the electronic relaxation pathways of electronically excited canonical nucleobases responsible for their ultrafast internal conversion to the ground state and, thus, for their intrinsic photostability.[1-8] In 2015, it was demonstrated that the purine chromophore is not responsible for the ultrafast internal conversion of the excited state population to the ground state in purine nucleobases, but that the amino and carbonyl groups play important roles in enabling their photostability to ultraviolet radiation.[9] The photostability of adenine and guanine was shown to be controlled by the nature of the substituents and by their specific position on the purine chromophore. However, to date, very little is known about the electronic relaxation mechanism of the pyrimidine chromophore and about the role the non-substituted pyrimidine moiety may have played in the selection of the canonical nucleobases as the building blocks of life during the harsh UV-radiation conditions present in the prebiotic era. Early efforts focused on the characterization of the electronic states of pyrimidine by means of theoretical and/or experimental techniques,[10-18] and on a comparison of its electronic properties with other azabenzene derivatives.[19-23]

In this Letter, we combine multiconfigurational ab initio modeling of potential energy surfaces (PES) and femtosecond broadband transient absorption spectroscopy to reveal the electronic relaxation pathways and dynamics of the pyrimidine chromophore. The combination of computational and experimental techniques allows for an unprecedented level of detail[9, 24-26] to ultimately discern the role of the pyrimidine chromophore on the intrinsic photostability of the canonical nucleobases.

Figure 1 shows the absorption spectrum of pyrimidine in three different solvents superimposed with the vacuum CASPT2 absorption line spectrum (see also Table 1 and Supporting Information for computational details). Two primary absorption bands are observed between 225 to 350 nm. The lower-energy absorption band corresponds to the $S_0 \rightarrow S_1(n\pi^*)$ transition, and its maximum exhibits 18 and 23 nm shift to longer wavelengths in going from phosphate buffered saline (PBS) solution at pH of 7.4 (270 nm) to acetonitrile (288 nm) and cyclohexane (293 nm), respectively. This bathochromic effect is further supported by time-dependent density functional calculations reported in Figure S1, which show a direct correlation of the $S_0 \rightarrow S_1(n\pi^*)$ transition energy with the dielectric constant of the solvent. The band centered at 243 nm is insignificantly perturbed by the solvent environment and is assigned to the $S_0 \rightarrow S_3(\pi\pi^*)$ transition. In the gas phase, the centers of these two bands have been recently located at 287 (nπ*) and 240 nm (ππ*),[27] in satisfactory agreement with previous measurements[15,17,18] and with our gas phase predictions (see Table 1).

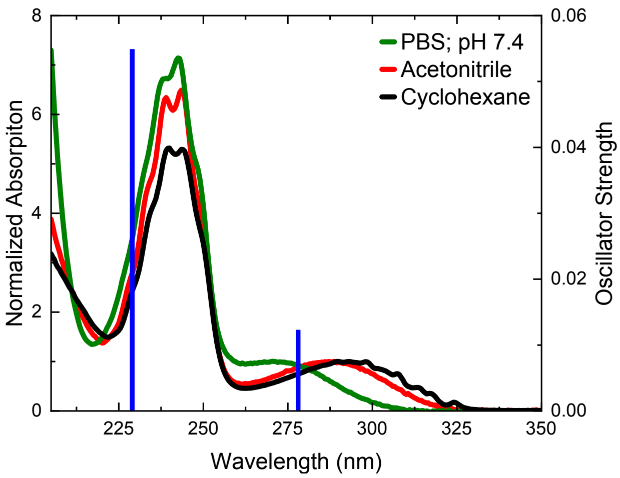

Figure 1. Normalized absorption spectra of pyrimidine in different solvents. Blue lines represent the vertical MS-CASPT2 excitation energies (see Table 1).

Table 1. Vertical excitation energies and oscillator strengths for the three singlet and two triplet lowest-energy excited states of pyrimidine at the MS-CASPT2/ANO-L level of theory in vacuum

State	ΔE / eV (nm)	Osc. Strength
S_1 (nπ*)	4.46 (278)	0.0123
S_2 (nπ*)	4.73 (262)	0.0000
S_3 (ππ*)	5.41 (229)	0.0549
T_1 (nπ*)	4.06 (305)	---
T_2 (ππ*)	4.56 (272)	---

Time-resolved transient absorption spectroscopy was used to reveal the excited state dynamics of pyrimidine. Figure 2 shows the experimental spectra for a pyrimidine concentration of 0.014 M in acetonitrile. Following excitation at 268 nm, two absorption bands are observed with similar intensity within the instrument response function (IRF = 270 ± 50 fs) of the experimental setup (Figure 2a). One of the bands has an absorption maximum at a lower probe wavelength than 350 nm, while the other has a maximum around *ca.* 650 nm (UV and visible bands, hereafter). For a time-delay of up to *ca.* 40 ps, the UV band starts decaying, while the visible band red shifts and its amplitude increases simultaneously (Figure 2b). An apparent isosbestic point is observed around 605 nm. From *ca.* 40 ps to 3 ns, both UV and visible bands decay, while the visible band slightly broadens and red shifts, apparently exhibiting a maximum above 700 nm (Figure 2c). The latter transient species decays at a significantly longer timescale than the 3 ns time window of the spectrometer used in this work. Similar experiments performed at a pyrimidine concentration of 0.002 M are presented in Figures S15 and S16 in the SI (see also Figure S14 and discussion therein). The results of these two different concentrations are equal within experimental uncertainties, suggesting that formation of any putative aggregates in the 0.014 M solution are not concealing the excited-state dynamics of the pyrimidine monomer.

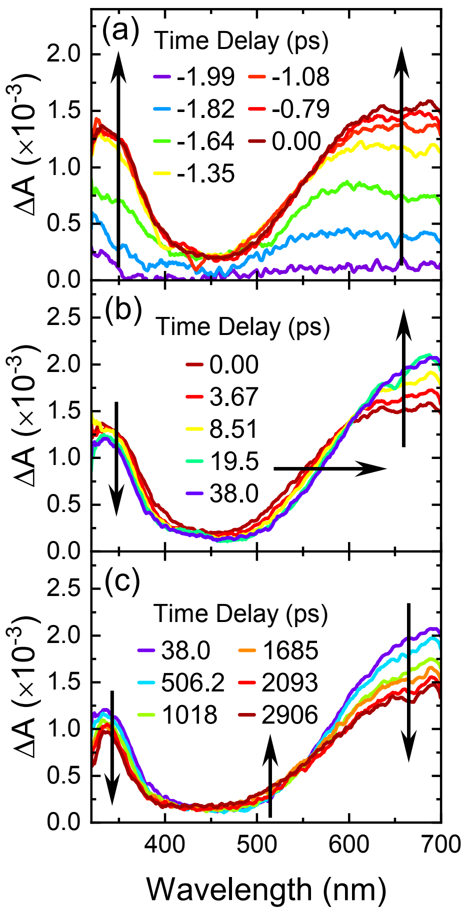

Figure 2. Transient absorption spectra for a pyrimidine concentration of 0.014M in acetonitrile excited at 268 nm.

Figure 3a shows representative decay traces and best global fit curves, extracted from a target and global analysis using a three-component sequential kinetic model, where the third kinetic component required a large lifetime (i.e., tens of ns) to satisfactorily fit the long-lived transient signal. The same analysis was performed for the data collected using a pyrimidine concentration of 0.002 M (see Figure S16 in the SI). These analyses yielded two set of lifetimes with averaged values of τ_1 = 7.8 ± 0.6 ps and τ_2 = 1.5 ± 0.8 ns. The extracted evolution associated difference spectra (EADS) are shown in Figures 3b and S16, respectively.

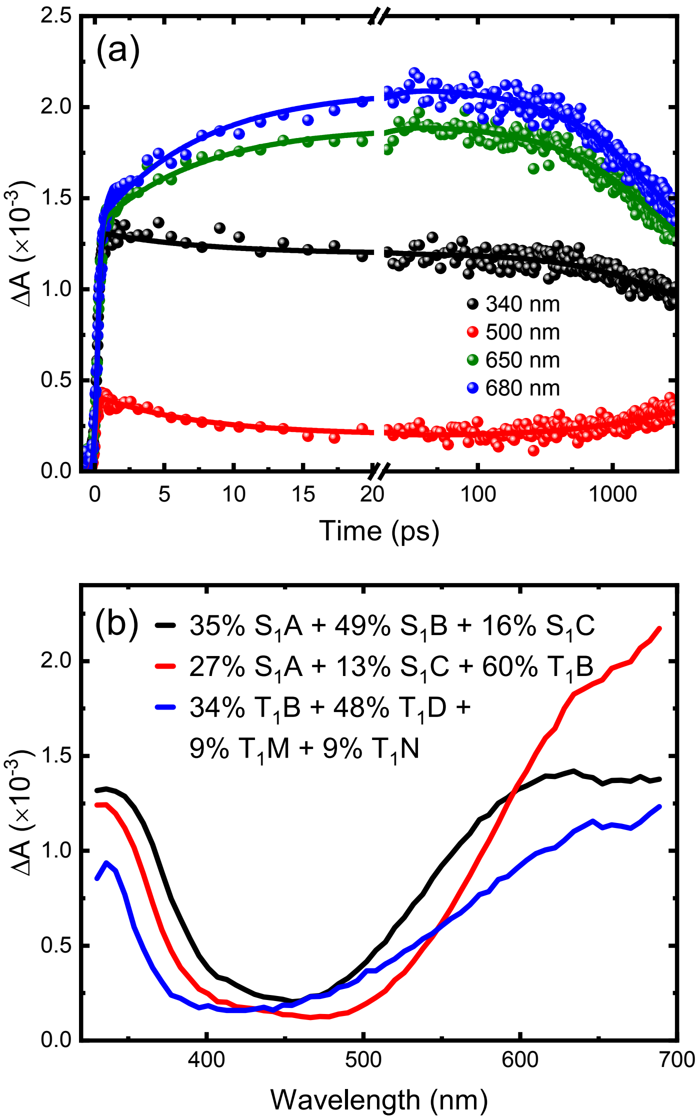

Figure 3. a) Selected kinetic traces of pyrimidine in acetonitrile excited at 268 nm. The fits represented are using a sequential kinetic model. b) Evolution associated difference spectra (EADS) and spectral assignments based on the quantum-chemical calculations: black EADS is assigned to $^1n\pi^*$ state (100%); red EADS is assigned to 40% $^1n\pi^*$ and 60% $^3\pi\pi^*$ states; and blue EADS is assigned to 18% $^3n\pi^*$ and 82% $^3\pi\pi^*$ states. See the main text and the Methods section in the SI for details.

In order to gain insight into the specific electronic relaxation pathways of the pyrimidine chromophore, the minimum energy paths, the singlet and triplet minima, the conical intersections and singlet-triplet intersystem crossing points (ICPs) of the PES reached upon excitation at 268 nm were optimized using multiconfigurational approaches (see SI for details). Figure 4 depicts the topography of the S_1 and T_1 PES and identifies key energy points and structures. Following excitation to the bright S_1 state, placed 4.43 eV above the ground state minimum,[28] the system is expected to populate the $^1n\pi^*$ minimum at 3.95 eV (labeled as S_1A in Figure 4), which preserves the planar structure of the ground state minimum with a small reduction of the N1-C2-N3 angle (See Inset of Figure 4 for atom labelling). Two other $^1n\pi^*$ minima are accessible from this minimum. The minimum at 4.00 eV (S_1B) has a planar, non-symmetrical structure (the reflection plane along the C2-C5 axis has disappeared), whilst the minimum at 4.04 eV (S_1C) shows a C2 puckered structure. The energy of the most stable minimum is consistent with the 0-0 energies estimated from the emission/excitation spectra (3.78 eV) and emission/absorption spectra (3.86 eV) in cyclohexane (see Table S2 and Figure S2). For these minima, we have located four different ground state decay funnels [S_1/S_0], which are labeled according to their distinctive geometry distortion on Figure 4: the affected carbon atom (C2 or C4) and the geometry rearrangement (U: Cx puckering + C-H bond perpendicular to the molecular plane; D: Cx puckering + C-H bond parallel to the molecular plane). Importantly, access to these $S_1 \rightarrow S_0$ crossings requires ascending upward potential energy profiles and/or surmounting energy barriers surpassing the initially available energy, and thus suggesting inefficient ground state repopulation.

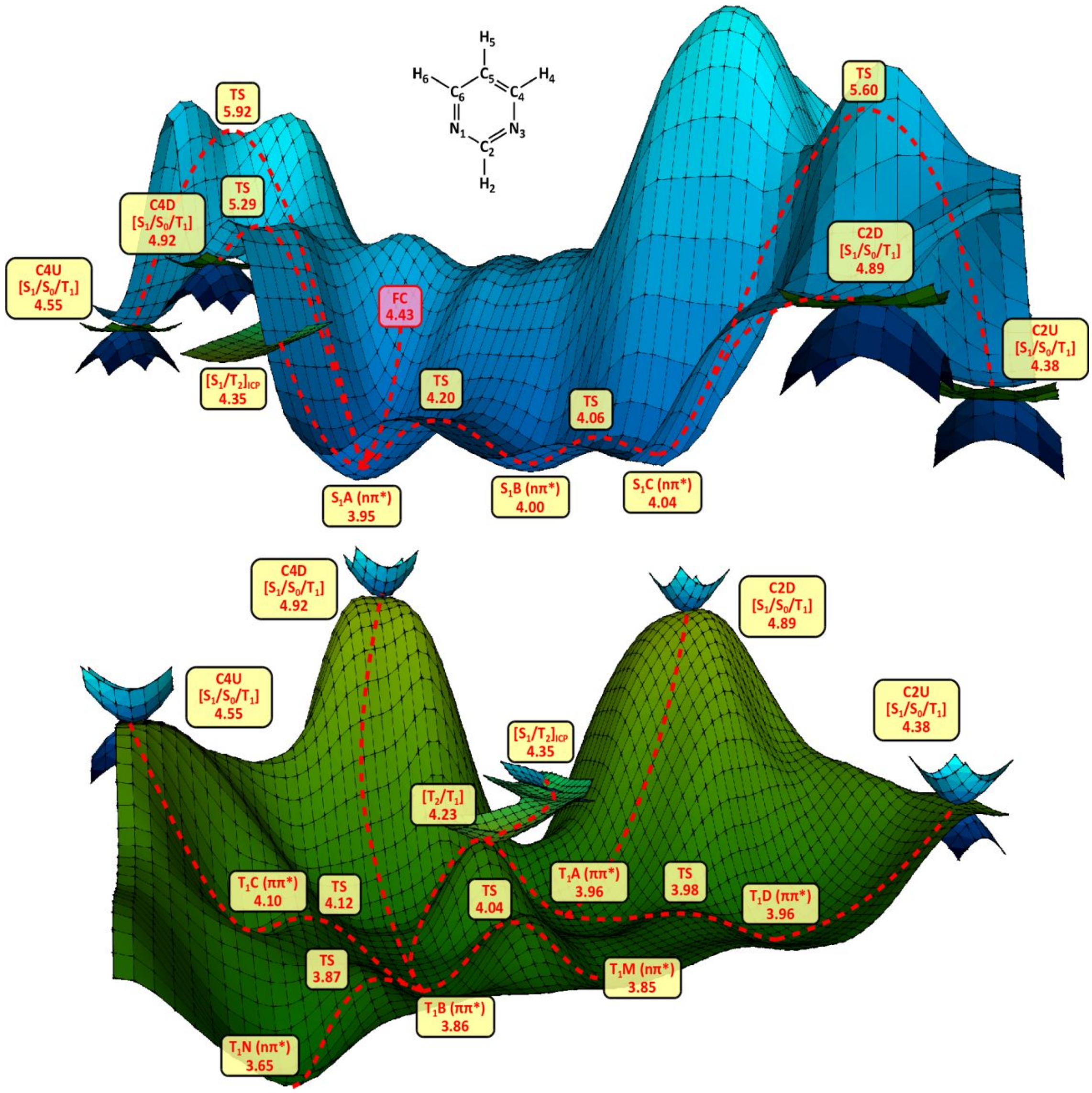

Figure 4. MS-CASPT2//SA-CASSCF(10,8) landscape of the S_1 (upper) and T_1 (lower) potential energy surfaces obtained from minimum energy path calculations (red lines); energies are given in eV relative to the ground state minimum. See SI for further information on the geometries.

Hence, we have investigated alternative relaxation pathways along the triplet manifold, which might be active for pyrimidine. In the vicinity of the S_1A minimum, we found a $[S_1/T_2]_{ICP}$ (4.35 eV), which requires almost no structural distortion, as it exhibits a planar structure. At this crossing point, we calculate a spin-orbit coupling of 8.6 cm^{-1}. This funnel is connected to a T_2/T_1 degeneracy point that would eventually lead to the population of two minima, T_1A and T_1B, which are connected to the T_1C, T_1D, T_1M and T_1N minima through relative low energy barriers. The intersystem crossing funnels that would allow for the leak of population from the triplet manifold to the ground state coincide in geometry and energy with the S_1/S_0 crossing points defined above, as they effectively correspond to $[S_1/S_0/T_1]$ triply-degenerate crossing points.

Among all the [$S_1/S_0/T_1$] intersystem crossing points, the most relevant one is the C2U (4.38 eV), as it is located slightly below the FC S_1 energy (4.43 eV). Hence, considering the calculated potential energy landscape, we propose that the primary electronic relaxation mechanism of pyrimidine would involve the following pathway: $S_1^* \rightarrow S_1A$ (+ S_1B, S_1C) $\rightarrow [S_1/T_2]_{ICP} \rightarrow [T_2/T_1] \rightarrow T_1B$ (+ T_1A, T_1D) $\rightarrow$ C2U-[$S_1/S_0/T_1$] $\rightarrow S_0$.

In order to provide further support to the proposed electronic relaxation mechanism, we have calculated the transient absorption spectra for all the minima shown in Figure 4 that are expected to be populated following excitation at 268 nm (4.63 eV) and, thus, to contribute to the transient spectra. The calculated individual spectra (see Figures S3 to S11 in the SI) were linearly combined to best fit the EADS reported in Figure 3b (Figure S13). Within the IRF of the experimental setup (Figure 2a), only the singlet minima contribute to the spectrum (see black EADS in Fig. 3b and Figure S13A), because they are easily accessible from the Franck-Condon region according to the topography of the PES, and all of them are required to reproduce the band from *ca.* 550 to 700 nm in terms of both width and intensity. With a lifetime of 7.8 ps (τ_1), intersystem crossing to the triplet manifold starts to ensue, as the main contribution to the EADS arises from the most stable $^3\pi\pi^*$ minimum (see red spectrum in Fig. 3b and Figure S13B), although the population of the S_1 minima is not negligible, which can be attributed to the energy barrier separating the singlet minima from the singlet-triplet funnel and/or the small spin-orbit coupling calculated at the S_1/T_2 crossing region. In this case, the S_1A and S_1C minima are necessary to reproduce the absorbance around 700 nm, whereas the absorption of T_1B is necessary to reproduce the signal from *ca.* 500 to 650 nm. Finally, the excited-state population partially decays within a lifetime of 1.5 ns (τ_2), and the EADS depicted in blue in Figure 3b is assigned to a contribution of triplet minima (see Figure S13C), which eventually decays to the ground state in a nanosecond to microsecond time scale.[11] In aqueous solutions, the long-lived triplet state of pyrimidine has been reported to decay back to the ground state in 1.4 μs.[11] The triplet quantum yield of pyrimidine in water has been reported to be near unity,[11] but it is significantly lower in organic solvents. In fact, a triplet quantum yield of 12% has been reported for pyrimidine in *n*-hexane,[29] which leaves about 88% of the initial population available to relax through other competitive pathways.

In this Letter, a comprehensive theoretical and experimental study of the photophysics and dynamics of pyrimidine chromophore is presented. Upon excitation at 267 or 268 nm, different minima in the $S_1(n\pi^*)$ PES are populated. On the picosecond time scale, a considerable fraction of the population intersystem crosses to the $T_1(\pi\pi^*)$ state, because the S_1/T_2 crossing and T_2/T_1 internal conversion funnels require negligible rearrangement in geometry from the preceding minimum, in contrast to the S_1/S_0 channels. Finally, population at the $^3\pi\pi^*$ minimum is able to survive for more than 3 ns. Excitation of cytosine, thymine, and uracil monomers at 267 nm primarily decay by ultrafast internal conversion to the ground state in hundreds of femtoseconds.[30-31] Small yields of long-lived $^1n\pi^*$ and $^3\pi\pi^*$ states are also observed in solution,[32-37] which decay back to the ground state in hundreds of picoseconds to few microseconds, respectively.

Collectively, it can be concluded that the pyrimidine core common to cytosine, thymine, uracil and other non-canonical pyrimidine derivatives is not the responsible for their ultrafast internal conversion to the ground state. The population of a long-lived triplet state suggests that the pyrimidine chromophore should have significantly lower photostability than the canonical nucleobases, which is in line with a recent proposal that photolysis plays an important role in the removal of pyrimidine from the troposphere.[27] The long-lived triplet species arises from the inaccessibility of internal conversion funnels, which are governed by distortions at the C2 and C4/C6 positions, which in pyrimidine happen to be equivalent by symmetry. Therefore, we propose that different substitution patterns over those atoms are critical to tune both the optical properties and the deactivation pathways of these nucleobases. In fact, a comparison of the gas phase absorption spectrum of pyrimidine with those of the canonical pyrimidine nucleobases uracil, thymine and cytosine, reveals that carbonyl C2 substitution and carbonyl or amino C4 substitution redshift (*ca.* 0.2-1 eV) the maximum of the most intense absorption band, being the effect of the amino group the greatest.[38-41] An intermediate shift (0.7 eV) in the maximum of the most intense absorption signal is observed upon the fusion of an imidazole ring to the pyrimidine core at the C4 and C5 positions, i.e., purine heterocycle, whilst the nπ* transition decreases its energy by 0.4 eV. The N-H bonds at the N1 (cytosine) or N1/N3 (uracil/thymine) positions block the dynamics from the nπ* state, characteristic of the pyrimidine core. Instead, in the canonical nucleobases, the lowest-lying ππ* state, responsible for the absorption maximum and controlled by barrierless potential energy profiles connecting the FC region with CI funnels to the ground state, governs their photophysics. This is in contrast to the potential energy landscape predicted for purine where, similarly to pyrimidine, the S_1(nπ*) potential acts as a doorway for the population of the triplet manifold.[9]

Supporting Information

The Supporting Information is available free of charge at:

Computational details, Steady-state properties of pyrimidine, Coordinates of relevant geometries of the potential energy surface, Theoretical transient absorption spectra for the minima, Theoretical Evolution Associated Difference Spectra and Experimental Methods.

Acknowledgements

This work has been supported by the Project PGC2018-094644-B-C21 of the Ministerio de Ciencia, Innovación y Universidades of Spain. I. C. and E. M. A. gratefully acknowledge the Ramón y Cajal program and a Formación de Profesorado Universitario contract from the Ministerio de Economía, Industria y Competitividad of Spain. The authors thankfully acknowledge the computer resources at Finisterrae and the technical support provided by the CESGA Supercomputing Center. Computational time from the Centro de Computación Científica (CCC) of Universidad Autónoma de Madrid and is also gratefully acknowledged. M.M.B., S.J.H., and C.E.C.-H. acknowledge the National Science Foundation (Grant No. CHE-1800052).

REFERENCES

1. Schreier, W. J.; Gilch, P.; Zinth, W., Early Events of DNA Photodamage. *Annu. Rev. Phys. Chem.* **2015,** *66*, 497-519.

2. Middleton, C. T.; de La Harpe, K.; Su, C.; Law, Y. K.; Crespo-Hernández, C. E.; Kohler, B., DNA excited-state dynamics: from single bases to the double helix. *Annu. Rev. Phys. Chem.* **2009,** *60*, 217-239.

3. Kleinermanns, K.; Nachtigallová, D.; de Vries, M. S., Excited state dynamics of DNA bases. *Int. Rev. Phys. Chem.* **2013,** *32*, 308-342.

4. de Vries, M. S.; Hobza, P., Gas-phase spectroscopy of biomolecular building blocks. *Annu. Rev. Phys. Chem.* **2007,** *58*, 585-612.

5. Beakstead, A. A.; Zhang, Y.; de Vries, M. S.; Kohler, B., Life in the light: nucleic acid photoproperties as a legacy of chemical evolution. *Phys. Chem. Chem. Phys.* **2016,** *18*, 24228-24238.

6. Stavros, V. G.; Verlet, J. R. R., Gas-phase femtosecond particle spectroscopy: a bottom-up approach to nucleotide dynamics. *Annu. Rev. Phys. Chem.* **2016,** *67*, 211-232.

7. Serrano-Andrés, L.; Merchán, M., Are the five natural DNA/RNA base monomers a good choice from natural selection? A photochemical perspective. *J. Photochem. Photobiol. C: Photochem. Rev.* **2009,** *10*, 21-32.

8. Callis, P. R., Electronic states and luminescence of nucleic acid systems. *Annu. Rev. Phys. Chem.* **1983,** *34*, 329-357.

9. Crespo-Hernández, C. E.; Martínez-Fernández, L.; Rauer, C.; Reichardt, C.; Mai, S.; Pollum, M.; Marquetand, P.; González, L.; Corral, I., Electronic and Structural Elements That Regulate the Excited-State Dynamics in Purine Nucleobase Derivatives. *J. Am. Chem. Soc.* **2015,** *137*, 4368-4381.

10. Cohen, B. J.; Goodman, L., Radiationless paths in the diazines. *J. Chem. Phys.* **1967,** *46*, 713-721.

11. Bent, D. V.; Hayon, E.; Moorthy, P. N., Chemistry of the triplet state of diazines in solution studied by laser spectroscopy. *J. Am. Chem. Soc.* **1975,** *97*, 5065-5071.

12. Carrabba, M. M.; Kenny, J. E.; Moomaw, W. R.; Cordes, J.; Denton, M., Hydrogen bonding in the lowest singlet n.pi.* excited state of pyrimidine. *J. Phys. Chem.* **1985,** *89*, 674-677.

13. Zeng, J.; Hush, N. S.; Reimers, J. R., Solvent effects on molecular spectra. II. Simulations of hydrated clusters and dilute solutions of pyrimidine in its lowest (n,π*) singlet excited state. *J. Chem. Phys.* **1993,** *99*, 1496-1507.

14. Fischer, G.; Cai, Z.-L.; Reimers, J. R.; Wormell, P., Singlet and triplet valence excited states of pyrimidine. *J. Phys. Chem. A* **2003,** *107*, 3093-3106.

15. Ferreira de Silva, F.; Almeida, D.; Martins, G.; Milosavljević, A. R.; Marinković, B. P.; Hoffmann, S. V.; Mason, N. J.; Nunes, Y.; Garcia, G.; Limão-Vieira, P., The electronic states of pyrimidine studied by VUV photoabsorption and electron energy-loss spectroscopy. *Phys. Chem. Chem. Phys.* **2010,** *12*, 6717-6731.

16. Linert, I.; Zubek, M., A study of the electronic states of pyrimidine by electron energy loss spectroscopy. *Chem. Phys. Lett.* **2015,** *624*, 1-5.

17. Stener, M.; Decleva, P.; Holland, D. M. P.; Shaw, D. A., A study of the valence shell electronic states of pyrimidine and pyrazine by photoabsorption spectroscopy and time-dependent density functional theory calculations. *J. Phys. B: At. Mol. Opt. Phys.* **2011**, *44*, 075203.

18. Bolovinos, A.; Tsekeris, P.; Philis, J.; Pantos, E.; Andritsopoulos, G., Absolute vacuum ultraviolet absorption spectra of some gaseous azobenzenes. *J. Mol. Spectr.* **1984**, *103*, 240-256.

19. Baba, H.; Goodman, L.; Valenti, P. C., Solvent effects on the fluorescence spectra of diazines. Dipole moments in the (n,π*) excited states. *J. Am. Chem. Soc.* **1966,** *88*, 5410-5415.

20. Dietz, T. G.; Duncan, M. A.; Puiu, A. C.; Smalley, R. E., Pyrazine and pyrimidine triplet decay in a supersonic beam. *J. Phys. Chem.* **1982,** *86*, 4026-4029.

21. Zhong, D. P.; Diau, E. W. G.; Bernhardt, T. M.; De Feyter, S.; Roberts, J. D.; Zewail, A. H., Femtosecond dynamics of valence-bond isomers of azines: transition states and conical intersections. *Chem. Phys. Lett.* **1998,** *298* (1-3), 129-140.

22. Reimers, J. R.; Cai, Z.-L., Hydrogen bonding and reactivity of water to azines in their S_1(n,π*) electronic excited states in the gas phase and in solution. *Phys. Chem. Chem. Phys.* **2012,** *14*, 8791-8802.
23. Chatterjee, S.; Wang, F., How different is pyrimidine as a core component of DNA base from its diazine isomers: A DFT study? *Int. J. Quant. Chem.* **2016,** *116*, 1836-1845.
24. Mai, S.; Pollum, M.; Martínez-Fernández, L.; Dunn, N.; Marquetand, P.; Corral, I.; Crespo-Hernández, C. E.; González, L., The origin of efficient triplet state population in sulfur-substituted nucleobases. *Nat. Commun.* **2016,** *7*, 13077.
25. Martínez-Fernández, L.; Granucci, G.; Pollum, M.; Crespo-Hernández, C. E.; Persico, M.; Corral, I., Decoding the molecular basis for the population mechanism of the triplet phototoxic precursors in UVA light-activated pyrimidine anticancer drugs. *Chem. Eur. J.* **2017,** *23*, 2619-2627.
26. Brister, M. M.; Crespo-Hernández, C. E., Excited-state dynamics in the RNA nucleotide uridine 5'-Monophosphate investigated using femtosecond broadband transient absorption spectroscopy. *J. Phys. Chem. Lett.* **2019,** *10*, 2156-2161.
27. Samir, B.; Kalalian, C.; Roth, E.; Salghi, R.; Chakir, A., Gas-phase UV absorption spectra of pyrazine, pyrimidine and pyridazine. *Chem. Phys. Lett.* **2020**, *751*, 137469.
28. Minimal discrepancies with Table 1 arise from the number of roots considered in the SA-CASSCF calculation.
29. Hochstrasser, R. M.; Marzzacco, C., Perturbations between electronic states in aromatic and heteroaromatic molecules. *J. Chem. Phys.* **1968**, *49*, 971.
30. Crespo-Hernández, C. E.; Cohen, B.; Hare, P.M.; Kohler, B. Ultrafast excited-state dynamics in nucleic acids. *Chem. Rev.* **2004**, *104*, 1977–2019.
31. Middleton, C. T.; de La Harpe, K.; Su, C.; Law, Y. K.; Crespo-Hernández, C. E.; Kohler, B. DNA excited-state dynamics: From single bases to the double helix. *Annu. Rev. Phys. Chem.* **2009**, *60*, 217–239.
32. Hare, P. M.; Crespo-Hernández, C. E.; Kohler, B. Internal conversion to the electronic ground state occurs via two distinct pathways for pyrimidine bases in aqueous solution. *Proc. Natl. Acad. Sci. USA* **2007**, *104*, 435–440.
33. Hare, P. M.; Crespo-Hernández, C. E.; Kohler, B. Solvent-dependent photophysics of 1-cyclohexyluracil: Ultrafast branching in the initial bright state leads nonradiatively to the electronic ground state and a long-lived $^1n\pi^*$ state. *J. Phys. Chem. B* **2006**, *110*, 18641–18650.
34. Hare, P. M.; Middleton, C. T.; Mertel, K. I.; Herbert, J. M.; Kohler, B. Time-resolved infrared spectroscopy of the lowest triplet state of thymine and thymidine. *Chem. Phys.* **2008**, *347*, 383–392.
35. Brister, M. M.; Crespo-Hernández, C. E. Direct observation of triplet-state population dynamics in the RNA uracil derivative 1-cyclohexyluracil. *J. Phys. Chem. Lett.* **2015**, *6*, 4404–4409.
36. Pilles, B. M.; Maerz, B.; Chen, J.; Bucher, D. B.; Gilch, P.; Kohler, B.; Zinth, W.; Fingerhut, B.P.; Schreier, W.J. Decay pathways of thymine revisited. *J. Phys. Chem. A* **2018**, *122*, 4819–4828.
37. Brister, M. M.; Crespo-Hernández, C. E. Excited-state dynamics in the RNA nucleotide uridine 5'-Monophosphate investigated using femtosecond broadband transient absorption spectroscopy. *J. Phys. Chem. Lett.* **2019**, *10*, 2156–2161.
38. Schreiber, M.; Silva-Junior, M. R.; Sauer, S. P. A.; Thiel, W., Benchmarks for electronically excited states: CASPT2, CC2, CCSD, and CC3. *J. Chem. Phys.* **2008**, *128*, 134110.
39. Serrano-Andrés, L.; Merchán, M. (2008) In: Shukla, M.; Leszczynski, J. (eds) Radiation induced molecular phenomena in nucleic acids. Springer, The Netherlands, p 435.
40. Lorentzon, J.; Fülscher, M. P.; Roos, B. O., Theoretical Study of the Electronic Spectra of Uracil and Thymine. *J. Am. Chem. Soc.* **1995**, *117*, 9265-9273.
41. Richter, M.; Mai, S.; Marquetand, P.; González, L., Ultrafast intersystem crossing dynamics in uracil unravelled by ab initio molecular dynamics. *Phys. Chem. Chem. Phys.* **2014**, *16*, 24423-24436.